Classification of Lateral Incisor Teeth for Aesthetic Dentistry Using Intelligent Techniques

Younis Samir Younis[1]*, Israa Mohammed Khudher[2]

[1]*Department of Computer Science, College of Computer Science and Mathematics, University of Mosul, Mosul, Iraq
[2]Department of Computer Science, Education College of Pure Sciences, University of Mosul, Mosul, Iraq

E-mail: [1]* fajirnet@gmail.com, [2] israa.alhamdani@uomosul.edu.iq

_____

Abstract

The six upper front teeth determine the appearance of Aesthetic dentistry. The study will define lateral incisors based on their lower angles as round, square, or square/round. LORIN molds to shape teeth were utilized. It extracted 144 teeth images from him and used 36 photographs of denture lateral incisors. The proposed work aims to develop a model capable of determining the most likely form the teeth will take. Intelligent systems first distinguish denture picture edges and separate gums from teeth. After early processing teeth were extracted. and use morphological methods performed to remove the hump, and The Savitzky-Golay filter then softens the corners. Images were tested to determine their type. Fuzzy logic determines the filter's mask size by finding the most matching teeth. we were cropped 50%, 66%, and 75% of the teeth and compared the rest lower parts of the teeth. Then, each type of tooth is matched using Pearson's correlation coefficient and LORIN-certified dental molds. When evaluating pictures of lateral incisor teeth, researchers found 36.1% accuracy when using the entire tooth, and 66.1% accuracy when cropping 75% of the tooth. The best match and discrimination of the lateral incisor were at cropping 50% and 66%, his accuracy was 86.1%. This study's results were compared to previous research on this subject, demonstrating their reliability and precision.

Keywords: digital smile design, Fully Convolutional Network, Convolutional Neural Network, Savitzky-Golay filter, LORIN dataset.

تصنيف الأسنان القاطعة الجانبية لتجميل الأسنان باستخدام تقنيات ذكية

يونس سمير يونس[1]*، اسراء محمد خضر[2]

[1]*قسم علوم الحاسوب ، كلية علوم الحاسوب والرياضيات ، جامعة الموصل، الموصل، العراق
[2]قسم علوم الحاسوب، التربية كلية العلوم الصرفة، جامعة الموصل، الموصل، العراق

المستخلص:

تحدد الأسنان الأمامية الست العلوية مظهر طب الأسنان التجميلي. ستحدد الدراسة القواطع الجانبية بناءً على زواياها السفلية على أنها دائرية أو مربعة أو مربعة / دائرية. سوف تستخدم قوالب لورين لتشكيل الأسنان. استخرجت منه 144 صورة أسنان واستخدمت 36 صورة

للقواطع الجانبية للأسنان. الهدف من العمل المقترح هو تطوير نموذج قادر على تحديد الشكل الذي ستتخذه الأسنان على الأرجح تميز الأنظمة الذكية أولاً حواف صور طقم الأسنان وتفصل اللثة عن الأسنان. بعد المعالجة المبكرة تم خلع الأسنان. واستخدمت الطرق المورفولوجية لإزالة النتوء، ثم يقوم مرشح Savitzky-Golay بتنعيم الزوايا. تم اختبار الصور لتحديد نوعها. يحدد المنطق الضبابي حجم قناع المرشح من خلال إيجاد الأسنان الأكثر مطابقة. قمنا بقص 50٪ و66٪ و75٪ من الأسنان وقارننا الأجزاء السفلية الباقية من الأسنان. بعد ذلك، تتم مطابقة كل نوع من الأسنان باستخدام معامل ارتباط بيرسون وقوالب الأسنان المعتمدة من LORIN. عند تقييم صور الأسنان القاطعة الجانبية، وجد الباحثون دقة 36.1٪ عند استخدام السن بالكامل، و66.1٪ دقة عند اقتصاص 75٪ من السن. أفضل تطابق وتمييز للقواطع الجانبية كانت في اقتصاص 50٪ و66٪، وكانت دقته 86.1٪. تمت مقارنة نتائج هذه الدراسة بالبحوث السابقة حول هذا الموضوع، مما يدل على موثوقيتها ودقتها.

الكلمات المفتاحية: تصميم الابتسامة الرقمية ، الشبكة التلافيفية بالكامل ، الشبكة العصبية التلافيفية ، مرشح Savitzky-Golay ، مجموعة بيانات LORIN.

---

1. Introduction

The doctor can utilize the Digital Smile Design (DSD) tool to create a beautiful smile for patients who are confident in the processing technique but unable to envisage the result of the therapy before it is performed. The goal of the DSD concept is to aid the clinician by enhancing the patient's aesthetic perception of their concerns, providing an understanding of the potential solution, and thereby educating and motivating the patient about the benefits of treatment while also increasing acceptance of the condition. A digital smile design is a digital model that helps in the construction and presentation of a new grin design by accomplishing simulation and a priori visualization of the proposed treatment's outcome. Patients are encouraged to participate in the process of designing their smiles as part of the digitally created design. This leads to the smile design being customized to the person based on their requirements and aspirations, which are then combined with the psychological features of the patient. It in turn improves their acceptance of the anticipated procedure and boosts their trust in the operation. [1].

Digital Smile Design (DSD) was developed with the intention of showcasing dentistry's more personal, emotional, and creative side to the rest of the world. as well as being more effective and accurate as a result of the use of digital technology, which further strengthens our respected role in the community. Digital Smile Design is a versatile conceptual dental treatment planning tool that is used in multidisciplinary aesthetic dentistry to enhance diagnostic vision and enhance predictability throughout the treatment period. Because a healthy, natural, confident, and beautiful smile is very important, Digital Smile Design was developed as a tool that could help achieve these goals. To develop an appropriate treatment plan for aesthetic dentistry, clinical data, study forms, and digital photographs are utilized. Even while these statistics are helpful for diagnosis, they do not give all of the information that is necessary for a comprehensive examination of the smile. As a result, the grin that was put is not the same as the smile that was taken on camera when the subject was moving. [2, 3]. This examination of the grin takes into account all of the parameters for shape and form. These parameters include the midline, the length of the upper incisors, the size of the teeth, the various shapes of the incisor teeth, and the way the size, texture, and transitional angles of the teeth look. Other parameters include the midline, the length of the lower incisors, the size of the teeth, and the different shapes of the incisor teeth [4].

No universally accepted scale can be used to measure the length of the teeth. As a result, it is essential to place a greater emphasis on models that are capable of producing the highest possible degree of congruence across the various forms. Following this, the best form of tooth that comes near to meeting the requirements of the system is identified. The kinds of teeth and their forms are determined by some different circumstances; nevertheless, the outside edges of the teeth on both sides are straight and parallel,

and they are situated in the region that is closest to the gums. Both the medial and distal outer edges of oval teeth are curved and thin in the region near the gums. This is due to the form of the oval teeth [2]. The cutting edge is somewhat rounded and rather thin. In the shape of triangular teeth, the perpendicular edge of the toothed border is not parallel to each other but is inclined, specifying that the region near the gum is thin with a broad, slightly curved incised edge. This is because the toothed border is in the form of a triangle. The lateral incisors have a form that is somewhere between an oval and a semi-oval, and they are positioned such that the gum line is centered on the long axis of the tooth. They are smaller than central incisors and have more rounded middle facial line angles, which is how they are distinguishable from those [5].

The main problem of this paper is to develop a model capable of determining the most likely form the teeth will take. This image is based on The LORIN mold database. This study helps the dentist to diagnose the teeth shape. This diagnosis detects the lateral incisors' shape based on their lower angles as round, square, or square/round. Based on dental image processing techniques. The main contributions of the paper are illustrated below:

- We use an artificial technique that supports dentists in making the correct diagnosis using dental photograph images.
- We semantically segmented the photograph images, and the gums were separated.
- We use morphological methods to remove the hump. We implement a refinement method to soften the corners.
- Then each tooth image is cropped to 50%, 66%, and 75% and compared to the rest lower parts of the tooth.
- We use fuzzy logic to determine the filter's mask size by finding the most matching teeth.
- Then, each tooth is matched using Pearson's correlation coefficient with LORIN-certified dental
- We estimate and compare the proposed solution with others formed for the same duty.

The rest of the paper is organized as follows: Section II discusses the related work. Section III contains details about the proposed work pipeline and its implementation. Section IV: contains The results discussion. While algorithmic quantitative evaluation are discussed in Section V. Section VI concludes the paper.

2. Related Studies

[3] The findings of an experiment to identify dental caries were given by M. T. Thanh, N. V. Toan, V. T. Nhu, N. T. Tra, C. N. Giap, and D. M. Nguyen. Applying Classical Esthetic Principles to Create a Predictable Illusion of Symmetry While Using Digital Technology. The experiment was done using training data consisting of 1902 photos, which were acquired from 695 individuals. The accuracy and classification rate of the results obtained by the four deep learning-adapted techniques are as follows: YOLOV3 (**You Only Look Once, Version 3**) with 83.4% and 60.7%, quicker R-CNN (**Region-based Convolutional Neural Network**) with 87.4% and 67.8%, Retinanet with 83% and 65.7%, and lastly SSD with 83% and 68.8% in year 2022. [4] V. Majanga and S. Viriri Automatic Blob Detection for Dental Caries, created a database of 11,114 teeth using dental radiographs by applying a Gaussian blur filter and utilizing erosion and dilation morphology. The study aimed to identify instances of dental caries, and the findings revealed the following information: The value for precision is equivalent to 97%, while the value for the recall is 96% in year 2021. [5] M. P. Muresan, A. R. Barbura, and S. Nedevschi, Teeth Detection and Dental Problem Classification in Panoramic X-Ray Images using Deep Learning and Image

Processing Techniques, made use of the CNN (**Convolutional Neural Network**) network in order to collect data from three different clinics. The researchers created a database consisting of 2,000 images from x-ray panorama films. The database was based on 1,000 images that were defined and labeled to indicate the type of image they were. The researchers separated the images into three categories: 70% training, 20% testing, and 10% cross-validation. The findings were correct 89% of the time in year 2020. [6] F. Schwendicke, K. Elhennawy, S. Paris, F. Philipp, and J. Krois, Deep Learning for Caries Lesion Detection in Near-Infrared Light Transillumination Images: A Pilot Study, classified 226 color photos using near- infrared light-transillumination images. The dimensions of the images were 435 by 407 Participants in the trial ranged in age from 8 to 11 years. Before being fed into the Resnet18 and Resnet50 neural network algorithms, the pictures were scaled up to a resolution of 224 pixels on each side. It had a sensitivity of 59% and a specificity of 76% giving it a detection accuracy of 74% in the year 2020. [7] A dental grading and the cutting process was provided on 87 photos by K. Moutselos, E. Berdouses, C. Oulis, and I. Maglogiannis Recognizing Occlusal Caries in Dental Intraoral Images Using Deep Learning. These researchers used several approaches (DNN (Deep Neural Network) Mask R- CNN, which extends Faster R-CNN by adding an FCN (**Fully Convolutional Network**) for predicting object masks). The findings demonstrated an accuracy of detection and categorization of 88.9%, and the ICDAS II (**International Caries Detection and Assessment System**) classification method was utilized to divide the findings into six distinct categories in 2019. [8] The faster R-CNN network was utilized by H. Chen, K. Zhang, P. Lyu, H. Li, L. Zhang, J. Wu, and C. Lee, A deep learning approach to automatic teeth detection and numbering based on object detection in dental periapical films. The number of dentures used in the experiments on X-ray films was 1250. The experiments were carried out. The data was separated into test datasets of 250, training datasets of 800, and validation datasets of 200. The results were in the matching phase of the detected data, which represented 868 out of 871 on the test dataset of 250, with a recall of 89.4% and a precision equal to 89.7%. The training datasets had a recall of 89.4% and a precision equal to 89.7% in 2019. [9] J. Lee, D. Kim, S. Jong, and S. Choi, Detection and diagnosis of dental caries using a deep learning-based convolutional neural network algorithm. worked together to gather 3,000 dental image graphs that were created using radiographic pictures. The pictures are separated into test data with 600 pictures, training and validation data with 2400 pictures. The training was carried out using the Google LeNet Inception v3 CNN network, in which the images were downsized to 299 x 299 pixels and represented as grayscale pictures with an accuracy of 82%, a sensitivity of 81%, and a specificity of 83%. in 2018. [10] M. Kim, B. Kim, B. Park, M. Lee, Y. Won, C. Kim, and S. Lee, A Digital Shade-Matching Device for Dental Color Determination Using the Support Vector Machine Algorithm, employed a digital shade- matching device. Because of the device's tiny size, the camera was able to be placed within the mouth, which was a significant advantage. This, in turn, stops the light from entering the mouth, allowing the picture to be captured with the highest possible level of precision, and allowing the user to manually specify the boundaries of the tooth in order for the support vector machine (SVM) algorithm to be used. A comparison was made between the findings and the Euclidean distance. The accuracy of the findings for the Euclidean distance came in at 77.3% for the corresponding device, while the SVM accuracy came in at 91.9%. These results were based on a total of 10 instances. In 2018. [11] Gil Silva, et al., Automatic segmenting teeth in X-ray images: Trends, a novel data set, benchmarking and future perspectives, presented ten dental segmentation methods on a dataset for X-ray camera model images (intra-oral or extra-oral) his a size of 2440 X 1292 pixels. A total of 1,500 photos were collected and organized into 10 distinct groups. Accuracy, Specificity, Precision, Recall, and F-Score are some of the metrics that were measured as part of the analysis. Regional growth accuracy was found to be 68.10 percent, splitting/merging at 81.07 percent, global thresholding at 79.29 percent, and the Niblack method at 81.82 percent. Additionally, fuzzy c-means (82.34%) outperformed canny (79.27%), Sobel (80.25%), without

edges (80.20%), the level set technique (76.37%), the watershed (76.58%), and the other methods (76.33%), In 2018. [12] Jae-Hong Lee, et al., Diagnosis and prediction of periodontally compromised teeth using a deep learning-based convolutional neural network algorithm, This paper presents the results of an investigation into a deep convolutional neural network (CNN) algorithm's potential use and accuracy in the detection and forecasting of periodontally compromised teeth (PCT). 1740 was imaged using a radiography dataset. There were 1044 used for training, 348 for testing, and 348 for validation. Accuracy, sensitivity, specificity, positive predictive value, and negative predictive value for diagnosis and prognosis, respectively. Additionally, the area under the ROC curve and the confusion matrix were analyzed to further assess the quality of the receiver operating characteristic (ROC) curve. periodontally compromised teeth (PCT) had an 81.0% diagnostic accuracy for premolars and a 76.7% accuracy for molars. The clinical comparison of these data revealed a precise extraction prediction of 82.8% for premolars and 73.4% for molars. In 2018. [13] Jie Yang, et al., Automated dental image analysis by deep learning on the small dataset, proposed a strategy for determining the effectiveness of dental care. Therek2 are 196 photos of dental X-rays taken at regular intervals that have been paired off for this data collection. That data was then divided into three categories: cases that improved, instances in which no changes were noticeable, and cases in which the condition worsened. All of these instances were labeled by seasoned dentists. A convolutional neural network (CNN) was trained using input from two standard adjacent areas. As a result of its efforts, the model for automated clinical quality assessment has an F1 score of 74.9%. in 2018. [14] Venkatesh, S. B., et al., Evaluation of recurring esthetic dental proportion in natural dentition with an esthetic smile, Statistical analysis of 100 photographs taken of Malaysian students smiling was provided. Determine the ideal dental proportion by comparing the average width of the maxillary central incisor to the average width of the maxillary lateral incisor, and the average width of the maxillary canine to the average width of the lateral incisor. Based on the data collected, the width of the maxillary lateral incisors ranges from 56.45 to 87.23%, with a mean value of 72.32%. Canine width as a percentage of lateral incisor width ranges from 49.15 to 88.67%, with the average coming in around 74%. In 2018. [15] F. Casalegno, et al., Caries detection with near-infrared transillumination using deep learning, in this study described a collection of 217 taken by near-infrared transmission (TI) photographs of upper and lower molars and premolars in grayscale. separated into There are 185 sak2mples used in the training phase and 32 in the validation phase. The data showed that, on average, an intersection over union (IOU) score of 72.7% was achieved. While the area under (AUR) curve was 83.6% for occlusion and 85.6% for proximal lesions. In 2019.

3. The Proposed Work Algorithm

The primary purpose of this effort is to develop a model that is capable of determining the most likely form that the teeth will take. The algorithm described in this work was used on an example of a tooth picture taken from a huge visual dataset known as LORIN [16, 17]. In addition, MATLAB R2021a is utilized in the execution of the application. The steps involved in the process of adapting the algorithm are shown in Figure 1. The development of the suggested algorithm requires multiple phases, which will be explained in the following order:
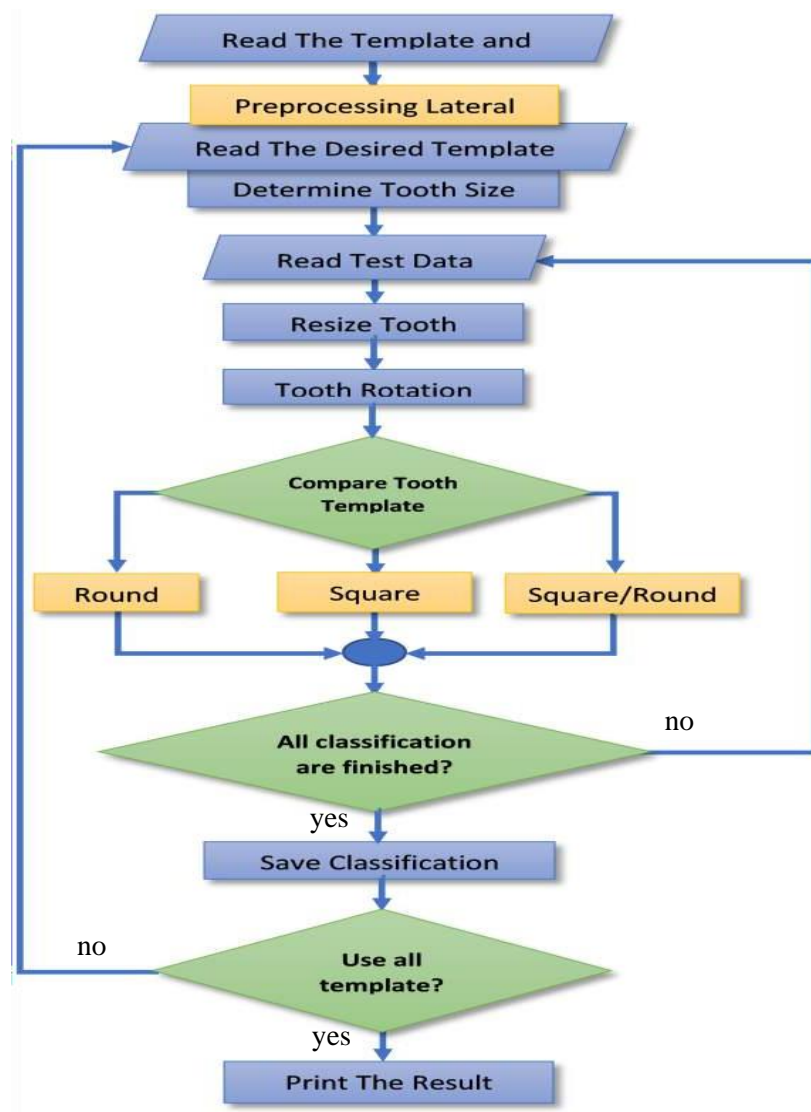
Figure 1. stages of the adapted algorithm

3.1.   Tooth Image Preprocessing

For this investigation, LORIN molds were utilized, and typical teeth were employed. Figure 2 displays a portion of the information contained in this database.
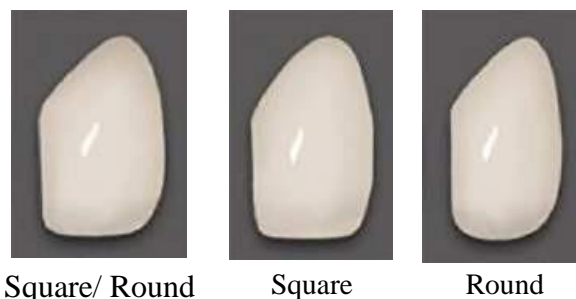

Square/ Round   Square   Round

Figure 2. Types of lateral incisor teeth with ideal shapes

These many kinds of teeth have been categorized and sorted beforehand. The lower border of each type of tooth is used as the primary criterion for classification, regardless of the overall shape of the tooth. The work axis that has been suggested can only take the form of a lateral incisor tooth (round) for either angle, a square (left)/round (right) for angles, or a square for both angles [18].

The information needed for the tests was collected from the teeth that were removed from the dentures depicted in figure 3.

Before process   After Square/Round-Square/Round-Round
Figure 3. Dental casts with processing

First, a series of initial processing operations that assisted in separating the gums from the teeth were carried out, and then the tooth was cut down from other teeth. as well as taking in the method that was used to categorize teeth as central incisors, lateral incisors, or cuspids was predicated on the number of pixels that were assigned to each tooth as well as the location of the tooth. After the scale of each tooth had been established using the Manhattan distance, the teeth were categorized using the K-NN clustering method [19]. Next Find the lower margins of each tooth, as this will be the method by which each tooth is differentiated from the others. Figure 3 depicts the outcome of segmenting the teeth, which was then followed by the selection of the lateral incisors for the further phases of the algorithm.

3.2. Recognition Evaluation Stage

Following the completion of the first steps, at which point the gums and teeth are separated from one another, the next step is isolating the individual teeth from one another. As can be seen in Figure 4, the size and positioning of the teeth led us to conclude that the tooth in question was the lateral incisor. When attempting to extract features from each tooth, the region props method is the one that is utilized. This method involved extracting the location of each shape within the dental picture, as well as its borders, area, mask, and color gradation, as well as "max Ferret Properties" and "min Ferret Properties" features. In the end, each tooth, even the right one, acquired traits that were unique to it.

3.3. Boundary Processing Stage

Figure 4 demonstrates that there is a distortion in the teeth's edges, which in turn causes the images to be deformed.
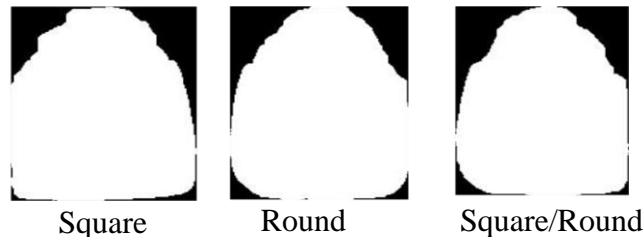

Square   Round   Square/Round
Figure 4. Lateral incisor teeth models

This can be seen as a direct result of the distortion in the teeth. In order to get rid of the deformation and change the contour of the tooth, a morphological procedure called an opening procedure was carried out. This procedure was represented by two processes called eroding and dilation. After that, the technology known as the Savitzky-Golay Filter was utilized to round down the sharp edges of the teeth,

and this process took place in a number of steps.

During these steps, the size of the mask is determined, and the convolution operation of the tooth image with the masker is made to conclude with a threshold that assists in maintaining the edge quality. After performing a number of tests and analyses on the tooth in terms of varying the size of the mask, fuzzy logic was utilized in order to select the best mask size by varying the size of the mask and matching the dental molds with the lateral incisor teeth that were segmented from the dentures. This was done after conducting a number of tests and analyses on the tooth. The size that is selected will have a one-to-one correspondence with the size of the tooth that was there to begin with, as evidenced by the percentage numbers in Table 1.

Table 1. Matching Frequency Based on Mask Size

No.	Mask size	Full	%75	%66	%50
1	1	9	6	8	9
2	10	6	9	10	10
3	20	11	15	12	12
4	25	12	24	27	27
5	30	13	24	31	30
6	35	9	21	13	24

Figure 5 Smoothing tooth edges for each type.
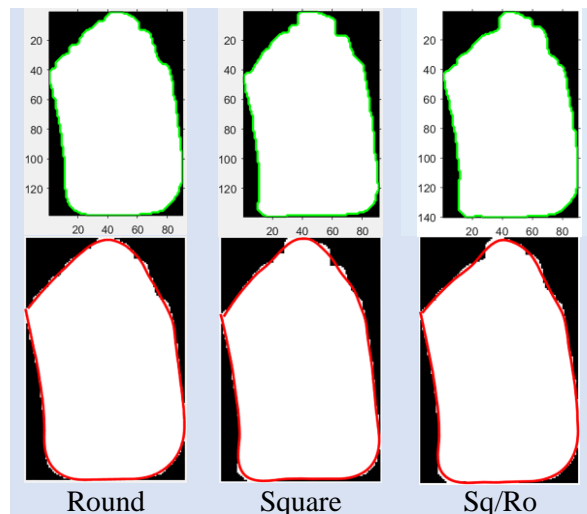

Round   Square   Sq/Ro

Figure 5. Resulting from smoothing edges

3.4. Tooth Rotation-Processing Stage

It follows one of the required processing stages for cutting the tooth horizontally, which is to rotate the tooth in the direction that the tooth is oblique, and the angle was determined by instructing region prop, which has feret properties. It follows one of the required processing stages for cutting the tooth horizontally, which is to rotate the tooth in the direction that the tooth is oblique. A tooth is shown both before and after it has been rotated in Figure 6.
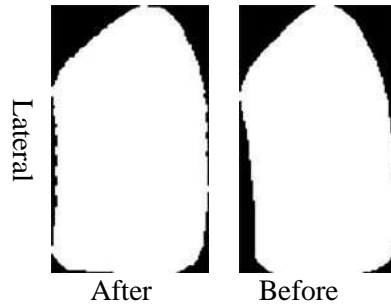
After   Before
Figure 6. Tooth rotation

Measurements of the length and width of the tooth are necessary for the process of identifying the lateral incisor teeth. These axes need to be identified, as their values have an impact on both the type of tooth and the resolute repair rate. Following this step is the procedure of cutting the tooth into three sections perpendicular to the cervical (c) teeth.

It denotes the portion that is close to the gum, and the gum is in close proximity to the upper side of it. after that comes the center, also known as the middle portion of the tooth. Thirdly, the incisal (l), which is the lowest part of the tooth, is the crucial element that was utilized in the process of locating and determining the type of tooth.

After the bottom portion of the lateral incisor tooth has been removed, the next component that has to be addressed is the contact surface, which has a significant bearing on the kind of lateral incisor tooth and its classification.

4.   The Outcomes Discussion

It was necessary to standardize the sizes of the teeth by making them the same size as the tooth mold in order to ensure that the results were consistent. This was accomplished by making the teeth the same size as the mold after the teeth had been extracted from a set of dental molds and the primary dental processes of morphologic treatment and edge smoothing had been finished. The stage of matching the dental molds with the teeth in the test data that was taken from the dentures has begun. This stage will continue until all of the teeth have been successfully matched. In each of the four stages of the experimental results of the Lateral Dental Test, the bottom part of the tooth is clipped and put through its paces for testing. The upper portion of the tooth is trimmed down by 75%, 66%, and 50% in order to perform a cropping surgery on the entire tooth. The remaining portion of the tooth is then used in the matching procedure. The Pearson's correlation coefficient, which was used in the paper to carry out the tests and is represented by equation 1 [20, 21], was utilized to complete the

$$r = \frac{n(\sum xy) - (\sum x)(\sum y)}{\left[n\sum x^2 - (\sum x)^2 \right]\left[n\sum y^2 - (\sum y)^2 \right]} \qquad (1)$$

n = number of values or elements.
x = 1st values list.
y = 2nd values list.

Figure 7 shows the best stability results obtained when the cutting rate is 50% and 66% for the mold and the test tooth, respectively. The reason is that these rates affect the shape of the tooth on the upper side and the percentage of connection with the neighbor, which gives high percentages of difference. When the lateral teeth were removed from the dentures, the results of this study revealed that they had lost

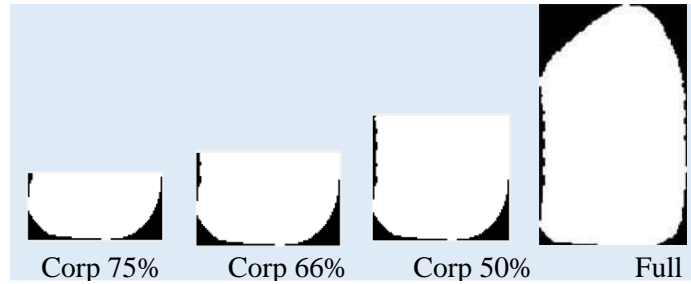one side of the mold due to the influence of the other teeth on this type of tooth (as depicted in Figure 7).

Figure 7. The cropped parts of the tooth

This was due to the fact that the other teeth had acted as a mold for the lateral teeth. This tooth loss is totally obvious from the left side as if it were a case of erosion, which in turn considerably influenced the variation of the results. It appears as though the tooth was worn away by erosion. Figure 8 depicts the process by which all of the test photos, totaling 144 extracts from him 36 lateral incisors teeth images, were read back into the template in which the results had been displayed. The results were obtained by analyzing four different versions of each photograph. These photographs are the first ones that completely capture what the tooth looks like. In the second image, the image is cut in half horizontally, and the lower portion of the image of the tooth is analyzed. The third representation is, in point of fact, that of the final third of the tooth.
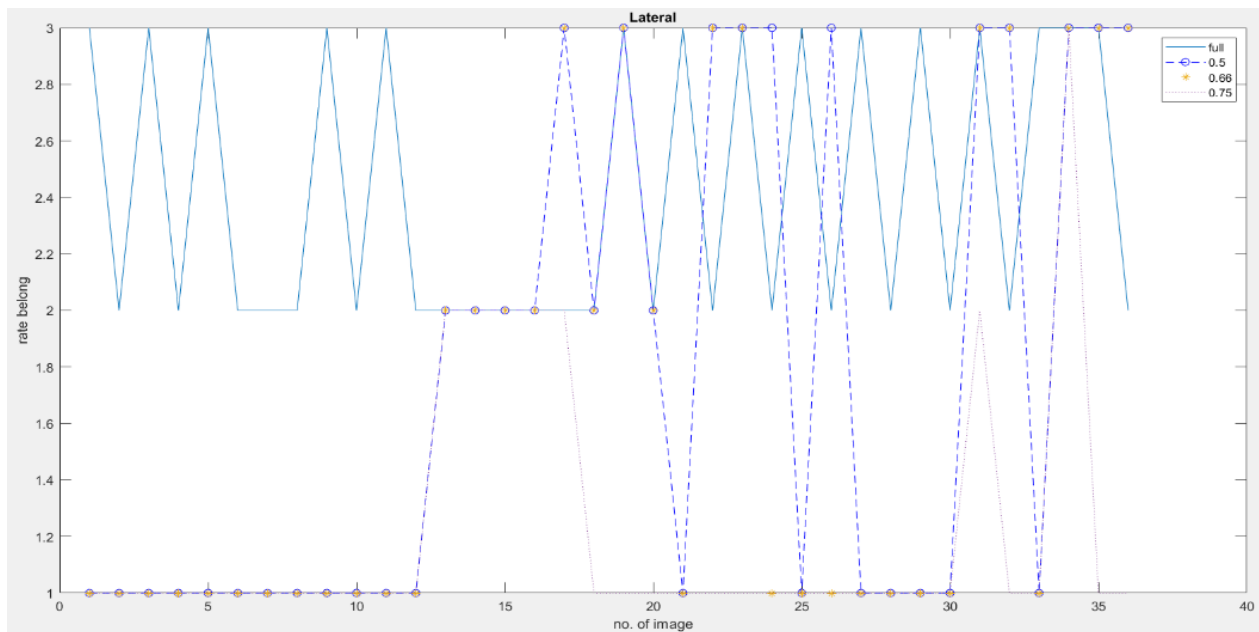

Figure 8. The images of the tested teeth and their corresponding

Figure 9 explains the percentage that demonstrates the connection of each of the 36 test photos to the corresponding model of the primary teeth. There were four different kinds of tests carried out: the first one looked at the tooth as a whole, while the second one split the image in half and focused on the lower half of it.
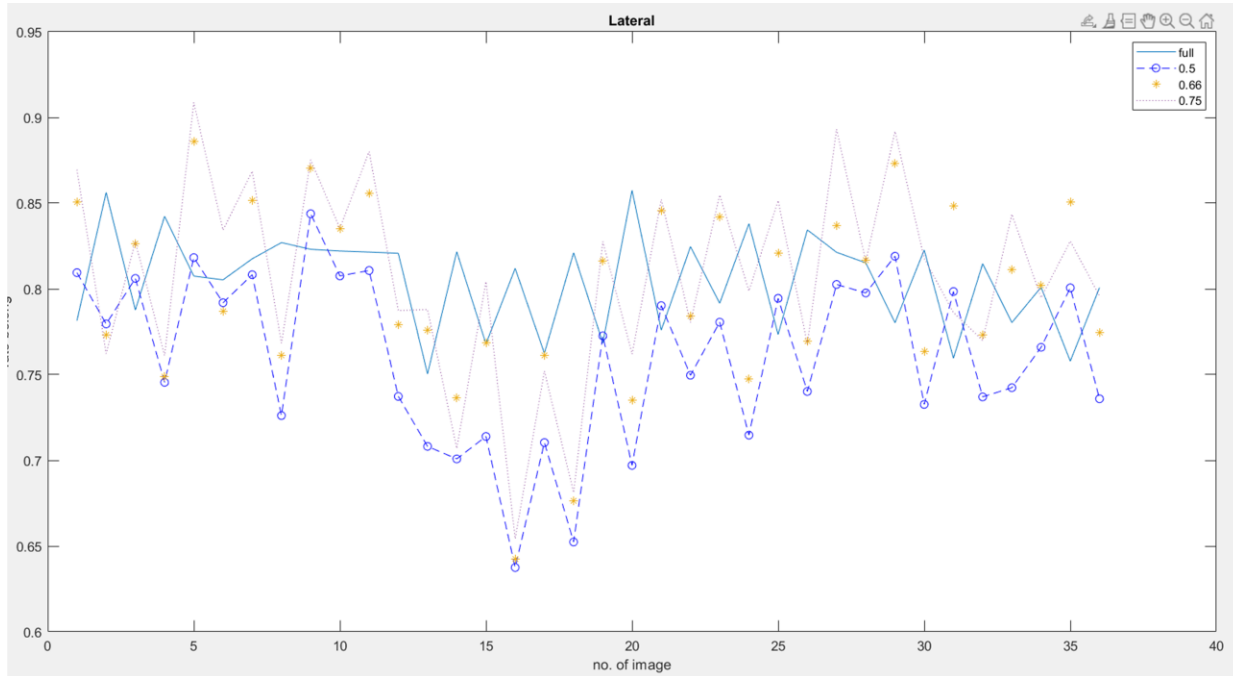
Figure 9. The strength of the test images' affiliation for each template

The final test examines the lower quarter of the tooth, while the third test focuses on the final third of the tooth's surface area.

The number of teeth present in the sample data is presented in Table 2, along with the total number of teeth for each category. These are the sorts that have rounded contours on the lower right and left corners of the tooth. The square is formed by joining the lower right and left corners of the teeth. In point of fact, there is a type of tooth (square/round) in which the two angles of the bottom tooth are distinct from one another. The angle that looks like a square is an angle that can be found close to the central incisor tooth on the opposite side. Concerning the circle, this component stands in for the aspect of each incisor tooth that is adjacent to or very close to the lateral tooth. This comes after the total number of teeth for each variety of tooth, as well as the rate of discovery for each variety, combined with the overall percentage of the tooth that remains after extraction.

Table 2. Types of teeth and the rate of discovery for each stage

No.	Type mold	Left tooth	Right tooth	Total	full	0.75	0.66	0.5
1	Round	9	9	18	0	18	18	17
2	square	3	3	6	6	5	5	5
3	Square/Round	6	6	12	7	1	8	9
Total		18	18	36	13	24	31	31
Rate					36.1%	66.6%	86.1%	86.1%

5. The Algorithm Qualitative Valuation

Four different measures were utilized in order to get an accurate picture of how effective and efficient the system was. These standards are referred to as the accuracy [9], which is demonstrated by the equation (2) and is defined as the proportion of accurate classifications.

$$Accuracy = \frac{(tp + tn)}{n} \qquad (2)$$

where tp is the number of images that have been appropriately identified, tn is the number of images that have been unequivocally rejected, and N is the total number of records in the database. The recall is the number of true positive cases for which the forecast was accurate, as demonstrated in equation (3) [23, 24].

$$Recall = \frac{TP}{(TP + FN)} \qquad (3)$$

where TP represents the number of photos that have been successfully identified and (TP+FN) represents the total number of images that have been correctly identified.

According to equation (4) [8] positive predictive value is a measurement of the accuracy of predicted positives in comparison with the rate of discovery of true positives. This is a measure of the accuracy of predicted positives.

$$PPV = \left(\frac{TP}{TP + FP} \right) \qquad (4)$$

We used to calculate the performance of the algorithm based on how balanced it was by the F-score, which combines precision and recall. This was done for the overall system quantitative criterion. When the numbers are quite similar, it attempts to estimate the average of the two. The harmonic average of precision and recall [25,25] is the function that the F-score is based on, as indicated in the equation below (5).

$$F1Score = 2*\left(\frac{Recall*PPV}{Recall + PPV} \right) \qquad (5)$$

In order to produce more accurate results and to demonstrate the affiliation of the teeth in a manner that is more understandable, tests were run on the data individually, and an experiment was carried out specifically on the data (round, square). In addition to these experiments, others were carried out on round, square, and round combinations, as well as square, square/round. All of these tests were carried out on the image of the tooth in its entirety, with cuts in percentages (50, 66, and 75), and Table 3 displays the total number of teeth that were found for each kind (round, square).

Table 3. Error classification rate for (round, square) edge

	Round, square Full	Round, square 0.75	Round, square 0.66	Round, square 0.5
TP	6	19	23	22
FP	10	5	0	0
TN	0	0	0	0
FN	8	0	1	2
Total	24	24	24	24

The round and square lateral incisor teeth, along with all of their performance evaluation measures, are depicted in Figure 10. It can be seen from the figure that the cut rate of 0.66 produces the best outcomes across all scales. This is followed by cut rates of 0.5 and 0.75, and the absolute worst results are obtained when the entire tooth is extracted.
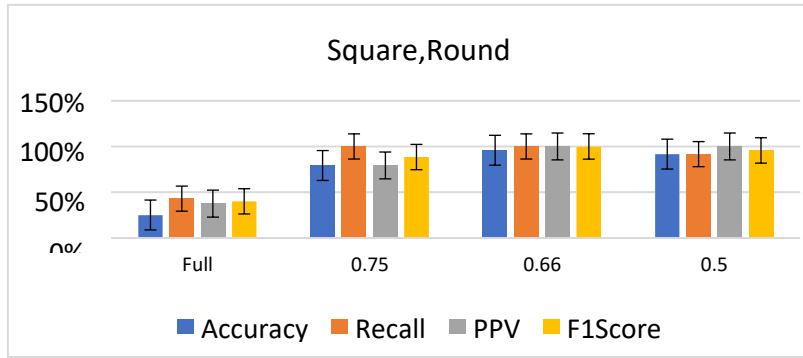
Figure 10. Performance Chart for tooth type square, round

The number of successfully identified and mistakenly identified teeth for the round, square/round (SR) type may be found in Table 4.

Table 4. Error classification rate for (round, square/round) edge

	Round, SR Full	Round, SR 0.75	Round, SR 0.66	Round, SR 0.5
TP	7	18	26	26
FP	8	0	3	3
TN	0	0	0	0
FN	15	12	1	1
Total	30	30	30	30

It is very evident that the error rate in the deceptive row, which depicts the percentage of incorrectly identified teeth, was lower in comparison to the number that should have been used.

A performance evaluation scale for the test data on tooth kinds (round, square/round) is presented in Figure 11. In comparison to the results of the last investigation, this one reveals a considerable drop. Once the tooth cut-off rate approaches 0.66, 0.75, then 0.5, and finally the ratio when the tooth is complete, the process is said to have converged.
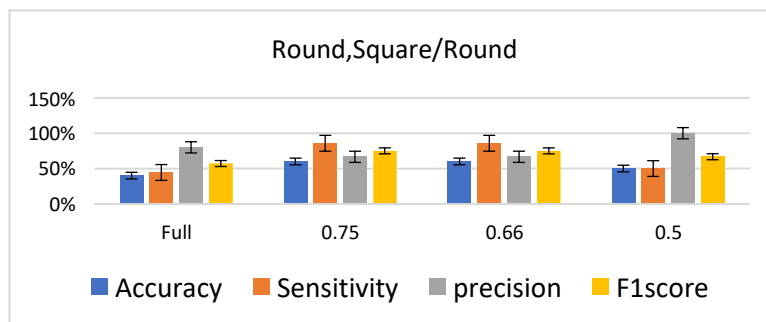

Figure 11. Performance chart for tooth type Round, Square/Round

The results of matching the teeth of the square and square/round types are presented in Table 5. The findings for the teeth that were discovered in the scenario represented by (Square, Square/Round) fared significantly better than the findings for the teeth that were discovered in the scenario represented by (Square, Round).

Table 5. Error classification rate for (Square, Square/Round) edge

	Square, S/R Full	Square, S/R 0.75	Square, S/R 0.66	Square, S/R 0.5
TP	13	11	13	13
FP	5	7	2	3
TN	0	0	0	0
FN	0	0	3	2
Total	18	18	18	18

Figure 12 illustrates the difference between square and square/round for each performance parameter. When the cut-off ratios (0.5 and 0.66) converge, the entire tooth is evaluated and 0.75 ratios are considered.
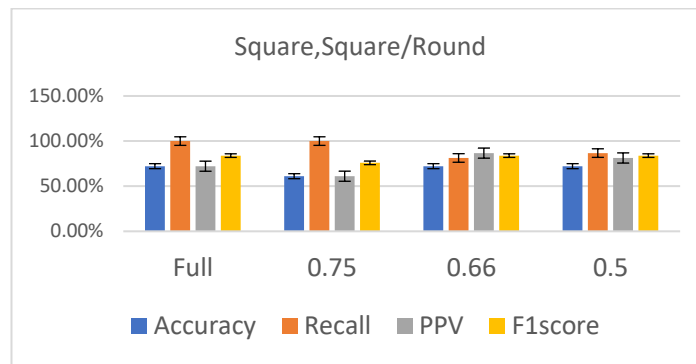

Figure 12. Performance chart for tooth type a Square, Square/Round edge

The comparison of the findings for the performance measure that was related to accuracy is presented in Table 6. The table demonstrates that the cut rate of 66% provides the highest level of precision for all different kinds of teeth.

According to the comparison that is displayed in Table 7, it was found that there is a decrease in performance when the teeth are fully adopted, but that performance gradually improves after each dental crop. It was also demonstrated that the findings produced had a connection to the teeth (round, square) when the crop was 66%, followed by 50%. This was the case.

Table 6. Accuracy scale Comparison

Types of Teeth	Performance evaluation metric		
	Acc. (R, S)	Acc. (R, S/R)	Acc. (S, S/R)
Full	25%	40%	72.2%
0.75	79.2%	60%	61.1%
0.66	95.8%	60%	72.2%
0.50	91.6%	50%	72.2%

Table 7. PPV scale comparison

Types of Teeth	Performance evaluation metric		
	PPV (R, S)	PPV (R, S/R)	PPV (S, S/R)
Full	37.5%	80%	72.2%
0.75	79.2%	66.6%	61.1%
0.66	100%	66.6%	86.7%
0.50	100%	100%	81.3%

These crops had the best overall results compared to others. In addition, there is an issue with the process of manufacturing square or round teeth (square/round), which are distinct sides of the tooth, as there is a significant mistake rate when comparing (round, square/round) teeth, making it difficult to discern between them. This problem stems from the fact that there is a high error rate when comparing the teeth between round and square/round, which led to the difficulty in distinguishing between them. When round teeth and square/round teeth were compared, the findings demonstrated that it was simple to

differentiate between the two types of teeth. However, when the comparison was done, it was determined that round teeth were superior to both square/round teeth and round/square teeth. The conclusion was those round teeth were the preferable option.

The PPV scale generated the best results across the board, and those findings were the same for both the square and round examples of the excised teeth, coming in at 66% and 50%, respectively. Additionally, a variety of values that was equal to 50% was found to be the poorest value for all scenarios when testing for the complete tooth as well as for round, square/round discontinuous teeth at this time. This was the case when testing for the complete tooth. This was the situation for the highest possible value of the crop. In spite of the fact that the findings varied according to the form of the teeth (square, square/round), it appeared that a reduction of the teeth by fifty percent produced the greatest outcomes for all of the participants.

Figure 13 shows that a cutoff of 66% delivers the best results for both square and round shapes, with a cutoff of 50% coming in second place. The results for round and square/round were volatile, but the results for square and square/round were quite close to the results for all cut-off instances and arrived in the second sequence of Square, Round. Despite the fact that it exhibited volatility in the results for round and square/round, the results for square and square/round were quite close to the results for all cut-off instances.
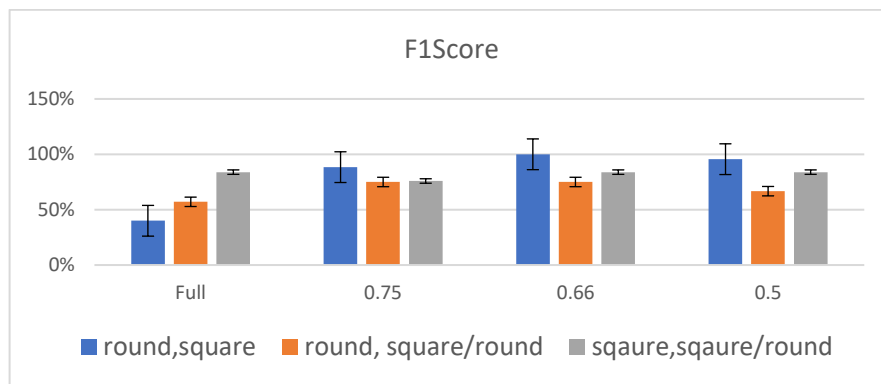

Figure 13 Performance chart for F-score

Figure 14 shows the receiver operating characteristics (ROC) analysis that was done to analyze the performance of the tested findings from true positives for tooth kinds. This study evaluated the performance of tested true positives. If the number is square/round, it means the finest production quality.
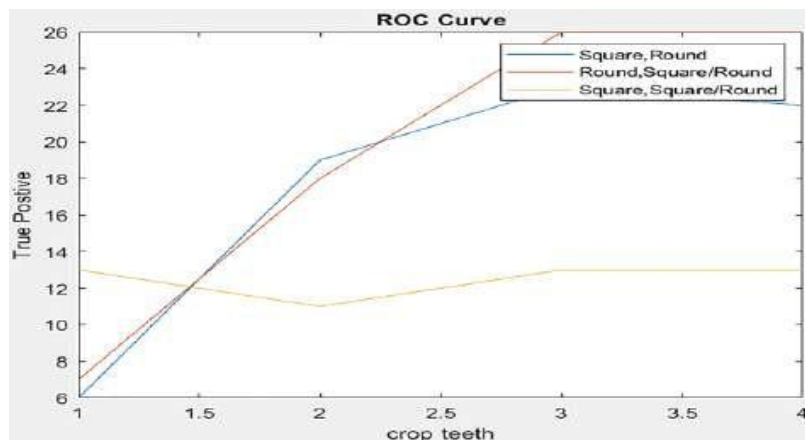

Figure 14. ROC Curve

Table 11 provides an explanation of the data that were achieved as well as a comparison of those results with other studies. The fact that the researchers have access to a vast quantity of X-rays and different sorts of images relevant to their research is the root cause to solve the problems. In addition to this, the resolution of the tooth image.

Table 11. Comparison with the related studies

Studies	Accuracy	No. of Image	Type of image
CNN [5]	89%	2000	x-ray films
Resnet18, Resnet50 [6]	74%	226	near-infrared light transillumination
Faster R-CNN + FCN [7]	89.7%	87	intraoral camera
YOLOv3(NSC vs. VNC) [3]	60.7%	1902	Mobile camera
Faster R-CNN (NSC vs. VNC) [3]	67.8%	1902	Mobile camera
RetinaNet (NSC vs. VNC) [3]	65.7%	1902	Mobile camera
SSD (NSC vs. VNC) [3]	68.8%	1902	Mobile camera
GoogLeNet Inception v3 CNN network [9]	82%	3000	radiographic images
SVM [10]	91.9%	10	Camera
Euclidean distance [10]	77.3%	10	Camera
Regional growth [11]	68%	1500	x-ray
deep convolutional neural network [12]	81%	1740	radiography
convolutional neural network [13]	74.9%	196	x-ray
Statistical analysis [14]	74%	100	photography
proximal lesions [15]	27.2%	217	near-infrared transmission
The proposed work	86.1%	136	Camera

6. Conclusion
The suggested work's objective is to achieve a high level of accuracy in the whole classification procedure. Because it was necessary to identify the type of lower tooth, the lower portion of the teeth had to be taken away, and matching procedures were carried out on them using either a third or a half. According to the research that has been done in the field of dentistry, a tooth should ideally be reduced in length by one- third, therefore it is typically segmented horizontally into three primary portions. The work that was proposed had a high level of accuracy when it came to the process of locating square or round types of teeth; however, it was unable to or did not contribute to the process of locating square or round teeth that have a different corner for the same tooth. This is because of a number of factors, one of which is the fact that the shape of the left part of the tooth, regardless of whether it is square or round, does not match the shape of the right part of the tooth, regardless of whether it is square or round. This is the case even though both parts of the tooth are classified as square or round. The application of fuzzy logic in the task that was proposed has demonstrated its value by producing very good outcomes in the process of matching. As a result, we strongly suggest that other researchers in this field make use of it in their work. In addition, the process of cutting the lower part of the teeth is divided into two vertical parts so that each corner may be addressed individually, and the smoothing operations can be carried out in a manner that is distinct from one another. Additionally, it is important to achieve better borders that are comparable to the required borders.

7. Acknowledgments

8. References

[1] Z. Jafri, N. Ahmad, M. Sawai, N. Sultan, and A. Bhardwaj, "Digital Smile Design-An innovative tool in cosmetic dentistry", *Journal of Oral Biology and Craniofacial Research*, vol. 10, no. 2, pp. 194-198, 2020, https://doi.org/10.1016/j.jobcr.2020.04.010.

[2] J. Bassett, "Applying Classical Esthetic Principles to Create a Predictable Illusion of Symmetry While Using Digital Technology", *Compendium of continuing education in dentistry*. Vol. 41, no. 4, pp. 204-210, 2020.

[3] M. Thi Giang Thanh, N. Van Toan, V. Truong Nhu Ngoc, N. Thu Tra, C. Nguyen Giap, and D. Minh Nguyen, "Deep Learning Application in Dental Caries Detection Using Intraoral Images Taken by Smartphones", *Applied Sciences*, vol. 12, no. 11, pp. 1-10, 2022, https://doi.org/10.3390/app12115504.

[4] V. Majanga, and S. Viriri, "Automatic Blob Detection for Dental Caries", *Applied Sciences*, Vol. 11, no. 19, pp. 1-12, 2021, https://doi.org/10.3390/app11199232.

[5] M. Paul Muresan, A. Răzvan Barbura, and S. Nedevschi, "Teeth Detection and Dental Problem Classification in Panoramic X-Ray Images using Deep Learning and Image Processing Techniques", *in: 2020 IEEE 16th International Conference on Intelligent Computer Communication and Processing*, pp. 457-463, 2020, 10.1109/ICCP51029.2020.9266244.

[6] F. Schwendicke, K. Elhennawy, S. Paris, P. Friebertshäuser, and J. Krois, "Deep Learning for Caries Lesion Detection in Near-Infrared Light Transillumination Images: A Pilot Study", *Journal of Dentistry*, vol. 92, pp. 1-5, 2020, https://doi.org/10.1016/j.jdent.2019.103260.

[7] K. Moutselos, E. Berdouses, C. Oulis and I. Maglogiannis, "Recognizing Occlusal Caries in Dental Intraoral Images Using Deep Learning", *in: 2019 41st Annual International Conference of the IEEE Engineering in Medicine and Biology Society (EMBC)*. 2019, pp. 1617-1620, 2019, 10.1109/EMBC.2019.8856553.

[8] H. Chen, K. Zhang, P. Lyu, H. Li, L. Zhang, J. Wu, and C. Lee, "A deep learning approach to automatic teeth detection and numbering based on object detection in dental periapical films", *Scientific Reports*, vol. 9, no. 1, pp. 1-11, 2019, https://doi.org/10.1038/s41598-019-40414-y.

[9] J. Hong Lee, D. Hyung Kim, S. Nyum Jeong, and S. Ho Choi, "Detection and diagnosis of dental caries using a deep learning-based convolutional neural network algorithm", *Journal of Dentistry*, vol. 77, pp. 106–111, 2018, https://doi.org/10.1016/j.jdent.2018.07.015.

[10] M. Kim, B. Kim, B. Park, M. Lee, Y. Won, Ch. Young Kim, S. Lee, "A Digital Shade-Matching Device for Dental Color Determination Using the Support Vector Machine Algorithm", *Sensors*, vol. 18, no. 9, pp. 1-13, 2018, http://dx.doi.org/10.3390/s18093051.

[11] Silva, G., Oliveira, L., & Pithon, M. "Automatic segmenting teeth in X-ray images: Trends, a novel data set, benchmarking and future perspectives". *Expert Systems with Applications*, vol. 107, pp. 15-31, 2018.

[12] Lee, J. H., Kim, D. H., Jeong, S. N., & Choi, S. H. "Diagnosis and prediction of periodontally compromised teeth using a deep learning-based convolutional neural network algorithm". *Journal of periodontal & implant science*, vol. 48, no. 2, pp. 114-123.

[13] Yang, J., Xie, Y., Liu, L., Xia, B., Cao, Z., & Guo, C. "Automated dental image analysis by deep learning on the small dataset". *IEEE 42nd Annual Computer Software and Applications Conference (COMPSAC)*, Vol. 1, pp. 492-497, 2018.;2

[14] Venkatesh, S. B., & Shetty, S. "Evaluation of recurring esthetic dental proportion in natural dentition with an esthetic smile". *Pak J Med Health Sci*, vol. 12, no. 4, pp.1867-1870, 2018.

[15] Casalegno, F., Newton, T., Daher, R., Abdelaziz, M., Lodi-Rizzini, A., Schürmann, F., ... & Markram, H. "Caries detection with near-infrared transillumination using deep learning". *Journal of dental research*, vol. 98, no. 11, pp. 1227-1233, 2019.

[16] H. Montaña Quintero, H. Montiel Ariza, and J. Reyes Mozo, "Performance Analysis for Algorithms of Recognition of Geometric Patterns in Mechanical Pieces", *International Journal of Applied Engineering Research*, vol. 12, no. 23, pp. 13807-13811, 2017.

[17] E. Itje Sela, and R. Pulungan, "Osteoporosis identification based on the validated trabecular area on digital dental radiographic images," *Procedia Computer Science*, vol. 157, pp. 282-289, 2019, https://doi.org/10.1016/j.procs.2019.08.168.

[18] L. Berland, and D. L. Traub, "Smile Style Chart," 2004, http://hauptlab.com/wp-content/uploads/2013/08/The-Smile-Guide.pdf.

[19] H. Çataloluk, and M. Kesler, "A diagnostic software tool for skin diseases with basic and weighted K-NN," *in: 2012 international symposium on innovations in intelligent systems and applications*, pp. 1-4, 2012, DOI: 10.1109/INISTA.2012.6246999.

[20] S. Yoon, H. Jung, J. C. Knowles, and H. Lee, "Digital image correlation in dental materials and related research: A review," *dental materials*, vol. 37, no. 5, pp. 758–771, 2021, https://doi.org/10.1016/j.dental.2021.02.024.

[21] A. Miranda Neto, A. Correa Victorino, I. Fantoni, D. E. Zampieri, J. V. Ferreira. D. A. Lima, "Image Processing Using Pearson's Correlation Coefficient: Applications on Autonomous Robotics," *in: 13th IEEE International Conference on Autonomous Robot Systems*, pp. 1-6, 2013, DOI:10.1109/Robotica.2013.6623521.

[22] I. Mohammed Khudher, Y. Ismail Ibrahim, "Swarm intelligent hyperdization biometric," *Indonesian Journal of Electrical Engineering and Computer Science*, Vol. 18, no. 1, pp. 385-395, 2020, http://doi.org/10.11591/ijeecs.v18.i1.pp385-395.

[23] Y. Ismail Ibrahim, I. Mahmmed Alhamdani, "A hyprid technique for human footprint recognition," *International Journal of Electrical and Computer Engineering (IJECE)*, vol. 9, no. 5, pp. 4060-4068, 2019, http://doi.org/10.11591/ijece.v9i5.pp4060-4068.

[24] I. Mohammed Khudher, "LSB Steganography Strengthen Footprint Biometric Template," *Восточно- Европейский журнал передовых технологий*, vol. 1, pp. 58-65, 2021, https://doi.org/10.15587/1729-4061.2021.225371.

[25] T. Xu, Y. Ma, K. Kim, "Telecom Churn Prediction System Based on Ensemble Learning Using Feature Grouping," *applies sciences*, vol. 11, no. 11, pp. 1-12, 2021, https://doi.org/10.3390/app11114742.